1985

Chronic Heart Failure Reduces Akt Phosphorylation in Human Skeletal Muscle: Relationship to Muscle Size and Function

Michael J. Toth
Kimberly Ward
Jos van der Velden
Mark S. Miller, *University of Massachusetts - Amherst*
Peter VanBuren, et al.

Chronic heart failure decreases cross-bridge kinetics in single skeletal muscle fibres from humans

Mark S. Miller[1], Peter VanBuren[1,2], Martin M. LeWinter[1,2], Joan M. Braddock[1], Philip A. Ades[2], David W. Maughan[1], Bradley M. Palmer[1] and Michael J. Toth[1,2]

Departments of [1] Molecular Physiology and Biophysics, and [2] Medicine, University of Vermont, College of Medicine Burlington, VT, USA

Skeletal muscle function is impaired in heart failure patients due, in part, to loss of myofibrillar protein content, in particular myosin. In the present study, we utilized small-amplitude sinusoidal analysis for the first time in single human skeletal muscle fibres to measure muscle mechanics, including cross-bridge kinetics, to determine if heart failure further impairs contractile performance by altering myofibrillar protein function. Patients with chronic heart failure ($n = 9$) and controls ($n = 6$) were recruited of similar age and physical activity to diminish the potentially confounding effects of ageing and muscle disuse. Patients showed decreased cross-bridge kinetics in myosin heavy chain (MHC) I and IIA fibres, partially due to increased myosin attachment time (t_{on}). The increased t_{on} compensated for myosin protein loss previously found in heart failure patients by increasing the fraction of the total cycle time myosin is bound to actin, resulting in a similar number of strongly bound cross-bridges in patients and controls. Accordingly, isometric tension did not differ between patients and controls in MHC I or IIA fibres. Patients also had decreased calcium sensitivity in MHC IIA fibres and alterations in the viscoelastic properties of the lattice structure of MHC I and IIA fibres. Collectively, these results show that heart failure alters skeletal muscle contraction at the level of the myosin–actin cross-bridge, leading to changes in muscle mechanics which could contribute to impaired muscle function. Additionally, we uncovered a unique kinetic property of MHC I fibres, a potential indication of two distinct populations of cross-bridges, which may have important physiological consequences.

(Received 22 April 2010; accepted after revision 16 August 2010; first published online 19 August 2010)
Corresponding author M. J. Toth: Health Science Research Facility 126B, 149 Beaumont Ave, University of Vermont, Burlington, VT 05405, USA. Email: michael.toth@uvm.edu

Abbreviations *A*, A-process magnitude; *B*, B-process magnitude; *C*, C-process magnitude; CSA, cross-sectional area; E_e, elastic modulus; E_v, viscous modulus; *f*, frequency of the length perturbations; *F*, force; *F*/CSA, tension; HF, heart failure; *k*, A-process unitless exponent; *L*, fibre length; L_{amp}, length oscillation amplitude; MHC, myosin heavy chain; MLC, myosin light chain; *n*, Hill coefficient; P_i, phosphate; *t*, time needed to perform length perturbations; t_{on}, average myosin attachment time; t_3, time from the start of stretch activation to the peak tension; $Y(\omega)$, complex modulus at peak calcium activation; ΔL, fibre length change; $\Delta L/L$, fibre strain; ω, $2\pi \times$ the frequency of the length perturbation; $2\pi b$, B-process characteristic rate; $2\pi c$, C-process characteristic rate.

Introduction

Heart failure is a clinical syndrome characterized by an inability of the heart to pump blood to meet the metabolic demands of the body. Accordingly, the most prominent symptom of the disease is a diminished capacity to perform physical work, which in turn contributes to high rates of disability (Pinsky *et al.* 1990). Although cardiac pump dysfunction is the primary etiological factor, adaptations in the peripheral musculature, including muscle atrophy (Toth *et al.* 1997), weakness (Harrington *et al.* 1997; Toth *et al.* In Press) and reduced oxidative capacity (Wilson & Mancini, 1993), contribute to functional limitations. Of these adaptations, the reduction in skeletal muscle contractile performance is of particular concern for the development of disability since it is a major determinant of the capacity to perform necessary activities of daily living (Bean *et al.* 2002). Thus, understanding the mechanisms underlying skeletal muscle contractile dysfunction in heart failure is important for developing strategies to maintain the functional independence of these patients.

Numerous studies have observed skeletal muscle weakness in heart failure patients that persists after controlling for muscle atrophy (Harrington *et al.* 1997;

 DOI: 10.1113/jphysiol.2010.191957

Toth *et al.* In Press). These findings in whole muscle are buttressed by studies in chemically skinned, single muscle fibres showing reduced contractile strength (i.e. tension) in both human heart failure (Szentesi *et al.* 2005; Miller *et al.* 2009*b*) and in animal models (van Hees *et al.* 2007), suggesting that alterations in myofilament proteins contribute to contractile dysfunction. Studies have further implicated a reduction in myosin heavy chain (MHC) protein content as a potential mechanism underlying muscle weakness (Toth *et al.* 2005; van Hees *et al.* 2007; Miller *et al.* 2009*b*). That is, muscle force production is reduced in heart failure because of a decrease in myosin protein content per unit muscle fibre size. Whether these quantitative alterations are further compounded by qualitative changes in myofilament protein function in heart failure, however, is not clear. Using the *in vitro* motility assay (filament sliding velocity), animal models suggest that heart failure alters the intrinsic function of skeletal muscle myosin (Coirault *et al.* 2007), while similar experiments in humans by our laboratory showed no effect of heart failure on skeletal muscle myosin or thin filament function (Okada *et al.* 2008). Using chemically skinned fibres, stretch activation experiments in animals indicate altered cross-bridge kinetics (van Hees *et al.* 2007), in agreement with recent circumstantial evidence from human fibres (Miller *et al.* 2009*b*). To date, no study has investigated possible changes in skeletal muscle cross-bridge kinetics resulting from human heart failure.

Small-amplitude, sinusoidal length perturbation analysis has been used to assess cross-bridge kinetics in a variety of muscle types, from insect flight (Miller *et al.* 2009*a*) to human cardiac (Mulieri *et al.* 2002). This experimental approach, with its high signal-to-noise ratio, enables measurement of myofilament protein function at the most basic unit of contraction, the myosin–actin cross-bridge. Importantly, these measurements are conducted while myofilament proteins are within their native, three-dimensional structure and are subjected to physiological loading conditions, both of which can alter cross-bridge kinetics. During a sinusoidal experiment, small, constant-amplitude, sinusoidal length perturbations, below the unitary myosin step size, are applied at a variety of frequencies and the tension response is measured. Elastic and viscous moduli are calculated for each oscillation frequency by determining the tension components that are in-phase and out-of-phase with the strain, respectively. Under Ca^{2+}-activated conditions, these moduli data provide information about the mechanical properties of the muscle and its components, and can be modelled to relate to specific steps of the cross-bridge cycle (Kawai *et al.* 1993; Zhao & Kawai, 1993; Mulieri *et al.* 2002; Palmer *et al.* 2007). Although this approach has provided insights into the basic physiology of skeletal and cardiac muscle in a variety of vertebrates (Kawai *et al.* 1993; Zhao & Kawai, 1993; Palmer *et al.* 2004; Galler *et al.* 2005), including human cardiac muscle (Mulieri *et al.* 2002), to our knowledge, it has never been applied to human skeletal muscle fibres.

In the present study, we report the first application of sinusoidal perturbation analysis to single human skeletal muscle fibres to examine the effects of chronic heart failure on cross-bridge kinetics. We evaluated single muscle fibres from the vastus lateralis muscle of patients with chronic heart failure and compared the results to sedentary controls. Of note, we experimentally controlled for the confounding effects of age and physical activity level on muscle function by matching patients and controls for these variables to ensure that the observed alterations in skeletal muscle cross-bridge kinetics are related to the heart failure syndrome, per se, rather than ageing or muscle disuse. We report that heart failure patients have slower cross-bridge kinetics and alterations in myofilament stiffness in MHC I and IIA fibres compared to controls, as well as decreased Ca^{2+} sensitivity in MHC IIA fibres. Additionally, we report a unique kinetic property of MHC I-containing muscle fibres; specifically, that there are potentially two distinct populations of cycling cross-bridges under isometric conditions, a phenomenon that has previously been observed in solution studies of MHC I skeletal muscle myosin (Iorga *et al.* 2007).

Methods

Ethical approval

Written informed consent was obtained from each of the fifteen volunteers prior to medical screening to rule out any conditions that may have precluded their participation. The protocol was approved by the Committees on Human Research at the University of Vermont and conformed to the *Declaration of Helsinki*.

Subjects

Nine patients (7 men, 2 women) with physician-diagnosed heart failure were recruited from the Heart Failure Clinic of the Cardiology Unit at the University of Vermont. The populations consisted of patients with systolic dysfunction (left ventricular ejection fraction $<40\%$; $n = 6$; range: 17–35%) and those with preserved systolic function (i.e. diastolic dysfunction; ejection fraction $>40\%$; $n = 3$; range: 45–52%), with an average ejection fraction of $33.6 \pm 3.9\%$. The average New York Heart Association (NYHA) functional class was 2.44 ± 0.18, with five class II patients and four class III patients. All patients were clinically stable and had not been hospitalized for 6 months prior to testing. None had signs or symptoms of severe hepatic (i.e. cirrhosis) or renal disease (i.e. plasma creatinine $>3\ \mathrm{mg\,dl^{-1}}$), peripheral vascular disease or an active neoplastic process and none

were smokers; however, three patients had Type II diabetes mellitus. All patients were on stable doses of heart failure medications, including angiotensin-converting enzyme inhibitors/receptor blockers (100%), β-blockers (89%) and diuretics (56%).

Controls ($n = 6$; 3 men, 3 women) were recruited who self-reported being sedentary to minimally physically active ($\leq$2 sessions of $\geq$30 min of exercise per week) and not currently participating in any organized exercise training or weight loss programs. Controls were also required to be non-smokers and have a stable body weight ($\pm$2 kg) for 6 months prior to testing. They had no signs or symptoms of heart failure, coronary heart disease or diabetes (fasting blood glucose $<112\,\mathrm{mg\,dl^{-1}}$), normal left ventricular function by echocardiography (ejection fraction >55%), normal blood counts and biochemistry values, and were not taking hormone replacement therapy (oestrogen or oestrogen/progestin therapy in women or testosterone in men). Data on whole muscle function and single fibre protein content and tension from some ($n = 12$) of the volunteers in this study have been published previously (Miller *et al.* 2009*b*; Toth *et al.* In Press).

Experimental protocol

Eligibility was determined during two screening visits at which time medical history, physical exam, blood samples, a treadmill test and echocardiography were performed. Muscle tissue was obtained the morning following an inpatient admission. Medications were maintained for all volunteers per normal dosing regimens prior to the inpatient visit, except coumadin in heart failure patients, which was stopped 5 days prior to admission. Volunteers were fasted after 19.00 h the evening of admission. On the following morning, muscle tissue was obtained via percutaneous biopsy of vastus lateralis muscle under lidocaine anaesthesia.

Peak oxygen consumption ($\dot{V}_{O_2,peak}$)

$\dot{V}_{O_2,peak}$ was determined using the Naughton protocol, as described previously (Ades *et al.* 2003).

Accelerometry

Free-living physical activity was estimated using a single-plane accelerometer (Caltrac; Muscle Dynamics Fitness Network, Torrance, CA, USA), as described previously (Ades *et al.* 2003).

Muscle tissue processing

Biopsy tissue was placed immediately into cold (4°C) dissecting solution (in mM: 20 *N*,*N*-*bis*[2-hydroxyethyl]-2-aminoethanesulfonic acid (BES), 5 EGTA, 5 MgATP, 1 free Mg^{2+}, 1 dithiothreitol and 0.25 phosphate (P_i) with an ionic strength of 175 mEq, pH 7.0, and at pCa 8 ($pCa = -\log_{10}[Ca^{2+}]$) for isolation of single fibres for mechanical measurements. Muscle fibres for mechanical measurements were dissected into bundles of approximately 50 fibres and tied to glass rods at slightly stretched lengths at 4°C and placed in skinning solution (in mM: 170 potassium propionate, 10 imidazole, 5 EGTA, 2.5 $MgCl_2$, 2.5 Na_2H_2ATP, 0.05 leupeptin and 0.05 antipain at pH 7.0) for 24 h at 4°C. After skinning, fibres were placed in storage solution (identical to skinning solution, but without leupeptin and antipain) with increasing concentration of glycerol (10% v/v glycerol for 2 h, 25% glycerol v/v for 2 h) until reaching the final storage solution (50% v/v glycerol), in which they were incubated at 4°C for 18–20 h. Thereafter, fibres were stored at −20°C until isolation of single fibres for mechanical measurements, which occurred within 4 weeks of the biopsy.

Preparation of single fibres for mechanics experiments

Segments (~2.5–3 mm) of single fibres were isolated from muscle bundles, aluminum T-clips were placed at both ends and the fibre mounted onto hooks in dissecting solution at 20°C. Fibres were fixed at two points approximately 1 mm apart with glutaraldehyde, as described elsewhere (Chase & Kushmerick, 1988; Hilber & Galler, 1998), with some modifications. Briefly, fibres were placed in rigor solution (in mM: 134 potassium propionate, 10 imidazole, 7.5 EDTA and 2.5 EGTA; 5 2,3-butanedione monoxime at pH 6.8) and glutaraldehyde fixative (4% toluidine blue (w/v), 30% glycerol (v/v), 2% glutaraldehyde(v/v)) was applied (20 s per end) using the gravity feed method (Hilber & Galler, 1998). The fibre was placed in dissecting solution with 1% bovine serum albumin to absorb any remaining glutaraldehyde (Chase & Kushmerick, 1988). New T-clips were placed on the fixed regions, which were evident because of toluidine blue indicator dye. Any fibre remaining outside of the fixed regions was cut off along with the original T-clips. The fibre was mounted onto hooks and top and side diameter measurements were made at three positions along the length of the fibre using a filar eyepiece micrometer (Lasico, Los Angeles, CA, USA) to calculate average cross-sectional area. The fibre was then incubated in dissecting solution containing 1% Triton X-100 (v/v) for 30 min at 4°C to ensure removal of sarcolemma and sarcoplasmic reticulum.

Experimental apparatus

An apparatus was constructed to allow performance of small-amplitude, sinusoidal length perturbations on

single, chemically skinned, skeletal muscle fibres and detection of corresponding force changes. This system is similar to that previously described by our research group for performance of sinusoidal analysis on cardiac and insect flight muscles (Mulieri *et al.* 2002; Miller *et al.* 2009*a*), but differs primarily in its method for changing the bathing solution, which was modelled after the approach described by Moss (1979). A flat, rectangular aluminum bath plate was constructed consisting of 13 wells (∼100 μl) to hold experimental solutions and a single large chamber (∼450 μl) for loading the fibre onto hooks attached to the force gauge and length motor. The plate was maintained at constant temperature by circulating cooling solution through channels milled into the chamber walls. The plate slides horizontally (*x*-axis) within a plastic trough, with each individual chamber being aligned to the longitudinal axis (*y*-axis) of the fibre by retractable ball bearings embedded in either side of the trough that fit into notches cut on either side of the plate. The bath plate and trough were mounted to an inverted microscope (Zeiss Invertiscope) so that it tracked vertically (*z*-axis) with the optics. The force transducer and length motor, in contrast, were attached to a fixed aluminum plate that served as the microscope stage. A portion of the stage was removed to accommodate the vertical displacement of the bath plate. To perform solution changes, the bath plate and optics were lowered using the coarse adjustment, which was modified to allow rapid movement in the vertical axis, and the bath plate was moved horizontally to the desired experimental solution. During solution changes, the time that the fibre was in the air was minimal (∼1 s).

Experimental solutions

Constituents of all solutions used during mechanical measurements were calculated using the equations and stability constants according to Godt & Lindley (1982). Relaxing solution was dissecting solution with 15 mM creatine phosphate and 300 units ml^{-1} of creatine phosphokinase. Pre-activating solution was the same as relaxing solution, except at an EGTA concentration of 0.5 mM. Activating solution was the same as relaxing solution, except at pCa 4.5. For single fibre measurements at 25°C, P_i levels were 5 mM to correspond with resting P_i levels in human skeletal muscle (Pathare *et al.* 2005). All solutions were adjusted to an ionic strength of 175 mEq using sodium methane sulfate.

Single muscle fibre mechanics

The T-clipped ends of the fibre were attached to a piezoelectric motor (Physik Instrumente, Auburn, MA, USA) and a strain gauge (SensorNor, Horten, Norway) in relaxing solution at 15°C, and sarcomere length set to 2.65 μm (IonOptix, Milton, MA, USA). To determine the length of the fibre's unfixed portion, since there is some longitudinal diffusion of the glutaraldehyde fixative into the fibre beyond the section stained with indicator dye (Chase & Kushmerick, 1988), the fixed portion of the fibre adjacent to each T-clip was determined by manually stretching (<2.5% fibre length) the fibre and monitoring sarcomere length (IonOptix). The fixed portion of the fibre showed minimal change in sarcomere length upon stretching. The fixed portion at either end was then subtracted from the total fibre length to obtain the unfixed fibre length (L).

Isometric tension measurements were performed at 15°C and 0.25 mM P_i, to correspond with previous studies in human skeletal muscle fibres (Yu *et al.* 1997; D'Antona *et al.* 2003; Trappe *et al.* 2003; Ochala *et al.* 2006, 2007), under relaxed (pCa 8) and maximal Ca^{2+}-activated (pCa 4.5) conditions. Starting in relaxing solution, the fibre was slackened completely, the force gauge zeroed, the fibre pulled back to its original position, allowed to equilibrate for 1 min and relaxed isometric tension measured. The fibre was transferred to pre-activating solution for 30 s and then to activating solution, with tension recorded at its plateau. Duplicate measurements of relaxed and maximal Ca^{2+}-activated tension were measured for each fibre. The Ca^{2+}-activated tension for each fibre was calculated as its maximal Ca^{2+}-activated tension minus relaxed tension.

Sinusoidal length perturbations and isometric tension measurements were performed at 25°C and 5 mM P_i, which corresponds with resting P_i levels in human skeletal muscle (Pathare *et al.* 2005), under maximal Ca^{2+}-activated conditions. During relaxed conditions, the fibre was slackened completely and the force gauge was zeroed. Thereafter, the fibre was pulled back to its starting position, allowed to equilibrate for 1 min and relaxed isometric tension measured. Following the 1 min equilibration period, the fibre was transferred to pre-activating solution for 30 s. The fibre was then transferred to activating solution (pCa 4.5) and, at the tension plateau, small-amplitude, sinusoidal length changes (0.05% or, in some cases, 0.125% of L) were applied to the fibre at 48 frequencies (0.25 to 200 Hz) while measuring the force response. Length and force were normalized to determine fibre strain ($\Delta L/L$) and tension (F/CSA) by dividing the length change (ΔL) by L and by dividing the force (F) by the fibre average cross-sectional area (CSA). Elastic (E_e) and viscous (E_v) moduli (kN m^{-2}) were calculated from the tension transient by determining the magnitudes of the in-phase and out-of-phase components (0 deg and 90 deg with respect to strain, respectively). The elastic and viscous moduli are the real and imaginary parts, respectively, of the complex modulus, the ratio of the tension response to the strain. Oscillatory work output was calculated

using work $= \pi ft(-E_v)(L_{amp})^2$ where f is the frequency of the length perturbations (Hz), t is the time needed to perform the perturbations (s), E_v is the viscous modulus (kN m^{-2}), L_{amp} is the length oscillation amplitude (i.e. 0.0005) and the unit of work is in kJ m^{-3}. Notably, a subset of maximally Ca^{2+}-activated fibres was examined under relaxed conditions using sinusoidal analysis and was found to produce small positive work values, indicating a population of cycling cross-bridges at this low Ca^{2+} level, a phenomenon we have also observed in human cardiac muscle (B. M. Palmer, unpublished observations). As both relaxed and maximally Ca^{2+}-activated conditions produce cycling cross-bridges, the relaxed results do not provide explicit insights into the passive fibre properties (absent cycling cross-bridges) and are therefore not included in this paper.

To relate sinusoidal analysis with specific steps in the cross-bridge cycle, the complex modulus at peak calcium activation was characterized by the following mathematical expression:

$$Y(\omega) = A(i\omega/\alpha)^k - Bi\omega/(2\pi b + i\omega) + Ci\omega/(2\pi c + i\omega), \quad (1)$$

where $\omega = 2\pi f$ in s^{-1}, A, B and C are magnitudes expressed in kN m^{-2}, $2\pi b$ and $2\pi c$ are characteristic rates expressed in s^{-1}, $i = -1^{1/2}$, $\alpha = 1$ s^{-1}, and k is a unitless exponent. For example, a Nyquist plot, or a plot of the viscous *versus* elastic modulus, for a human MHC I skeletal muscle fibre from a heart failure patient was fitted using the above equation (Fig. 1*A*) and broken down into its three processes (A, B and C). The A-process (described by parameters A and k) is a linear relationship between the viscous and elastic moduli, while the B-process (described by parameters B and b) and C-process (described by parameters C and c) are semi-circles (Fig. 1*B*). These six parameters have been related to various aspects of muscle mechanics through experimentation and modelling (Kawai *et al.* 1993; Zhao & Kawai, 1993; Mulieri *et al.* 2002; Palmer *et al.* 2007). Although different models vary in their precise interpretation, the following summarizes our current thoughts on the meaning of these parameters. The A-process has no kinetic or enzymatic dependence (Q_{10} of ~0.9; Mulieri *et al.* 2002) and reflects the viscoelastic properties of the structural elements of the fibre across the oscillation frequency range. Under fully relaxed conditions, where no myosin heads are attached, the A-process represents the viscoelastic properties of the underlying fibre structure. Under Ca^{2+}-activated conditions where myosin heads are attached, the A-process represents the underlying lattice structure, as well as a portion that increases with Ca^{2+} concentration that is ascribed to the attached myosin heads (Mulieri *et al.* 2002; Palmer *et al.* 2004). The parameter A indicates the magnitude of a viscoelastic modulus and k represents the angle at which the A-process lies relative to the x-axis. Thus, k reflects the viscous-to-elastic modulus relationship of the A-process. The magnitude part of the B-process (B) is proportional to the number of myosin heads strongly bound to actin and the cross-bridge stiffness (Kawai *et al.* 1993). The characteristic rate of the B-process ($2\pi b$) is hypothesized to represent the apparent (observed) rate of myosin force production or,

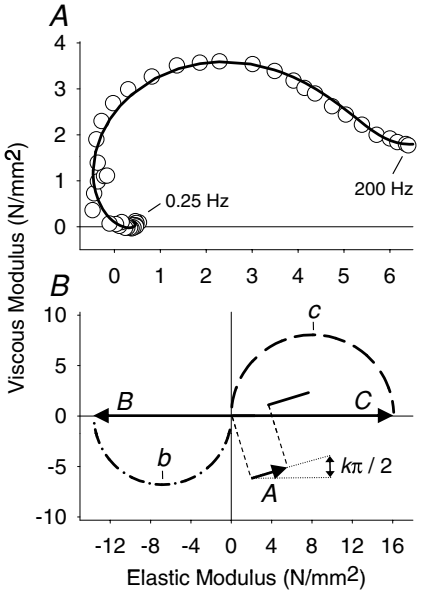

Figure 1. The six-parameter model used to fit the Nyquist plots produced by sinusoidal analysis
A, the Nyquist plot of a Ca^{2+}-activated (pCa 4.5) MHC I fibre, where each open circle represents one of the 48 oscillation frequencies (0.25 to 200 Hz) performed during sinusoidal analysis, provides information on the mechanical properties (elastic and viscous moduli) of the muscle fibre and its components. The sinusoidal analysis results (open circles) are well-characterized by the continuous line, calculated using a six-parameter model whose equation is in the text. *B*, the six model parameters, which can be related to cross-bridge function and myofilament structural properties, are paired into three different processes: the linear A-process (continuous line, described by parameters *A* and *k*), the semicircular B-process (dash–dot line, described by parameters *B* and *b*) and the C-process (dashed line, described by parameters *C* and *c*). As a negative viscous modulus indicates positive work production, the B-process is work producing and the A- and C-processes are work absorbing. The *B* and *C* parameters, displayed as arrows the length of the diameter of the semicircular B- and C-processes, are magnitudes (N mm^{-2}) proportional to the number of strongly bound cross-bridges and cross-bridge stiffness. The parameters *b* and *c* indicate the frequencies (Hz) at which the B- and C-processes exhibit viscous modulus values that are the most negative (or largest oscillatory work production) and positive (or largest oscillatory work absorption), respectively. Importantly, $2\pi b$ and $2\pi c$ are characteristic rates (s^{-1}) related to cross-bridge kinetics, with $(2\pi c)^{-1}$ being equivalent to myosin attachment time (t_{on}). The A-process represents the viscoelastic properties of the underlying lattice structure as well as strongly bound cross-bridges. The parameter *A*, represented by an arrow, indicates a magnitude (N mm^{-2}) and *k* (a unitless exponent) is the angle at which the A-process lies relative to the *x*-axis.

in other words, the rate of myosin transition between the weakly- and strongly-bound states (Zhao & Kawai, 1993). For the C-process, C is equivalent to the number of myosin heads strongly bound to actin multiplied by the cross-bridge stiffness, and is therefore proportional to B, and $(2\pi c)^{-1}$ represents the average myosin attachment time to actin, t_{on} (Palmer *et al.* 2007).

Ca^{2+} sensitivity

Tension–pCa curves were performed on a sub-set of the fibres used for sinusoidal analysis. These fibres were maximal Ca^{2+}-activated (pCa 4.5) once at 15°C, as described above, returned to relaxing solution and subsequently activated in solutions containing progressively higher Ca^{2+} levels (pCa 7, 6.5, 6, 5.75, 5.5, 5.25, 5, 4.5), with tension measured at each plateau. Individual recordings of normalized tension were fitted to the Hill equation $[Ca^{2+}]^n/([Ca^{2+}]_{50}{}^n + [Ca^{2+}]^n)$, where $[Ca^{2+}]_{50}$ is the calcium concentration at half-activation, pCa_{50} is the $-\log [Ca^{2+}]_{50}$ and n is the Hill coefficient.

Gel electrophoresis

Following all mechanical and Ca^{2+} sensitivity measurements, single fibres were placed in 30 μl loading buffer, heated for 2 min at 65°C and stored at −80°C until determination of MHC isoform composition by SDS-PAGE to identify fibre type, as described previously (Toth *et al.* 2005), with minor modifications. Briefly, 2.0 μm^3 of fibre volume (estimated from fibre length and cross-sectional area measurements) was loaded. The stacking gel contained 4% acrylamide/bis–5% glycerol (w/v) and the resolving gel 7% acrylamide/bis–30% glycerol (w/v). Gels were run at 70 V for 3.5 h, followed by 200 V for 20 h at 9°C. The gel was silver stained (BioRad) and the MHC isoform (MHC I, IIA and/or IIX) expressed in each single fibre was determined by comparison to a standard containing all MHC isoforms (Fig. 2*A*).

The myosin light chain (MLC) composition of a sub-set of single MHC IIA muscle fibres used for mechanics experiments described above was determined by SDS-PAGE (Fig. 2*B*). Samples were loaded (2.0 μm^3 of calculated fibre volume) on 12% polyacrylamide gels, which were run at constant current (25 mA) at 20°C till the dye front reached the bottom of the gel (∼1 h) and were then silver stained (Silver Snap; Pierce, Rockford, IL, USA). The position of each MLC band was determined using standards containing multiple single muscle fibres (i.e. expressing MHC I, IIA, IIX fibres) and myosin extracted from human skeletal muscle and cardiac tissue, as described previously (Okada *et al.* 2008). Gels were scanned and each MLC isoform band was quantified by densitometry (Quantity One, BioRad) and expressed as a molar fractional abundance by dividing the band intensity signal by its respective molecular weight (23 for MLC 1f, 17 for MLC 2f and 15 for MLC 3f) and expressing this value relative to the total MLC signal.

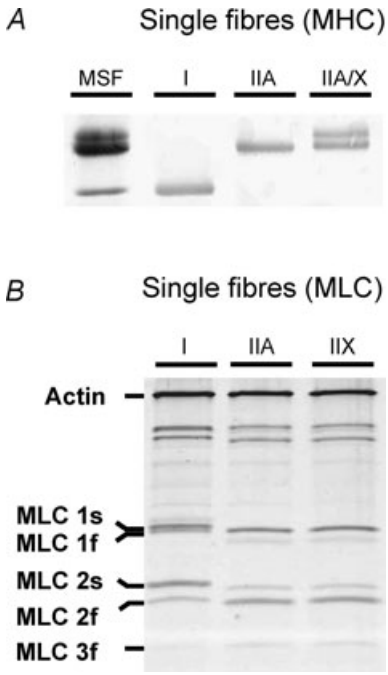

Figure 2. Representative MHC and MLC gels from single human skeletal muscle fibres
Silver-stained SDS-PAGE gels show separation of MHC (*A*) and MLC (*B*) isoforms. MSF, multiple single fibres.

Statistics

All data are reported as mean ± S.E.M. Two-sample Student's t tests were used to examine differences between control and heart failure groups for most variables, except for the elastic and viscous moduli since these were measured across different sinusoidal oscillation frequencies. For the moduli data, a repeated measures analysis was used, with frequency as a repeated measure, and pair-wise comparisons performed between the control and heart failure groups at each frequency. Relationships between variables were determined using Pearson correlation coefficients. All analyses were conducted with SPSS software version 16 (SPSS Inc.; Chicago, IL, USA).

Results

Subjects

Physical characteristics for heart failure patients and controls are shown in Table 1. Groups were similar for age, height, body mass and body mass index, although $\dot{V}_{O_2,peak}$ was lower ($P < 0.01$) in patients compared to controls.

Table 1. Clinical characteristics and physical activity levels of controls and heart failure patients

	Controls	Heart failure
Age (years)	70.7 ± 2.4	69.3 ± 4.4
Height (cm)	166.3 ± 5.3	173.9 ± 2.6
Body mass (kg)	88.9 ± 8.8	103.7 ± 9.4
Body mass index (kg m^{-2})	31.9 ± 2.2	34.0 ± 2.8
Peak oxygen consumption (ml kg^{-1} min^{-1})	23.3 ± 2.3	13.7 ± 1.0*
Physical activity level (kcal d^{-1})	254 ± 64	249 ± 46

Data are mean ± S.E.M. for $n = 6$ controls and $n = 9$ heart failure patients. Peak oxygen consumption data are expressed relative to body mass. *$P < 0.05$.

Daily physical activity level measured by accelerometry over an average of 7.5 ± 0.7 days did not differ between patients and controls.

Single muscle fibre mechanics

At the standard amplitude of 0.125% fibre length for the sinusoidal length perturbations applied to muscle preparations in studies carried out in our laboratory and others for insect flight (Miller *et al.* 2009*a*), cardiac (Mulieri *et al.* 2002; Palmer *et al.* 2004) and skeletal muscle (Wang & Kawai, 1997), we found a significant amount of non-linearity in the force response in MHC I human skeletal muscle fibres over a broad range of frequencies. To assure a linear force response, a requirement of our method of analysis, we reduced the amplitude of the applied sinusoidal length perturbations. We found that length changes of 0.05% fibre length resulted in a linear force response, while maintaining an adequate signal-to-noise ratio. Interestingly, this change in the amplitude of the sinusoidal length oscillations uncovered a unique characteristic of MHC I human skeletal muscle fibres. Figure 3*A* shows the characteristic Nyquist plot for MHC I fibres using 0.125% length amplitude, which is similar in form to that observed in MHC I fibres from rabbits (Wang & Kawai, 1997). Use of 0.05% length amplitude in MHC I fibres, however, revealed a 'notch' that typically occurred within the frequency range of 1 to 4 Hz (notch labelled at 2.75 Hz in Fig. 3*A*). Although decreasing the length perturbation amplitude had little effect on the Nyquist plot at oscillation frequencies below the notch (<2 Hz), the response to oscillation frequencies at and above the notch (2–200 Hz) are greatly affected by the change in amplitude (Fig. 3*A*). Importantly, this phenomenon is not unique to MHC I human skeletal muscle fibres. We have observed a similar notch phenomenon, at even larger perturbation amplitudes, in human cardiac tissue at 37°C (notch labelled at 4.5 Hz in Fig. 3*B*), which primarily expresses the identical MHC protein (i.e. β-MHC) as MHC I skeletal muscle fibres, and it has also been observed in embryonic isoforms of *Drosophila* muscle myosin (Yang *et al.* 2008). In contrast, this notch is not evident in MHC IIA (Fig. 3*C*), IIA/IIX or IIX fibres. We have recorded the frequency at which the notch occurs in order to evaluate the potential effect of heart failure. Patients with heart failure (HF) have a lower notch frequency ($P < 0.05$) compared to controls (control: 2.79 ± 0.07 *vs.* HF: 2.58 ± 0.07 Hz; $n = 84$ and 75 fibres, respectively).

In the present study, we have chosen to use the six-parameter curve fit to the Nyquist data (Fig. 1) to establish the primary effects of heart failure on single fibre mechanics and cross-bridge kinetics, assuming that t_{on} is represented by a single exponential probability function for the stochastic process that underlies $2\pi c$ (Palmer *et al.* 2007). Since the notch does not appreciably reduce our

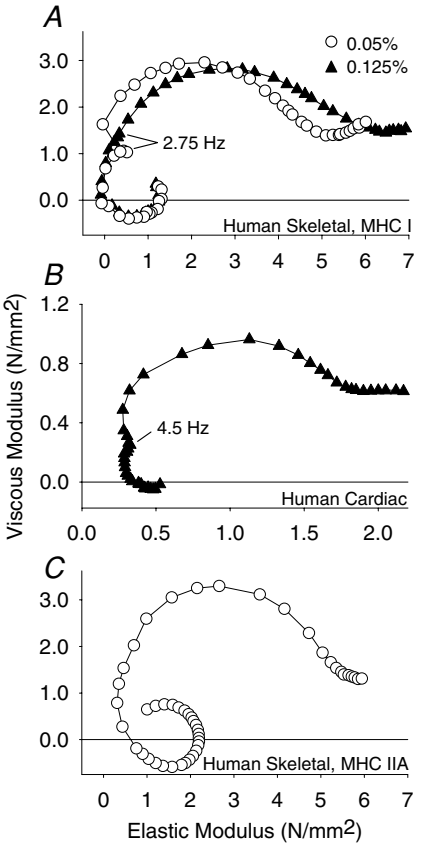

Figure 3. Representative Nyquist plots for Ca^{2+}-activated (pCa 4.5) single human skeletal muscle fibres and cardiac strips
A, an MHC I human skeletal muscle fibre at 25°C and 5 mM P_i with a muscle length perturbation amplitude of 0.05% produces a notch (labelled at 2.75 Hz), although no notch is observed when the perturbation amplitude is increased to 0.125%. *B*, a human cardiac muscle strip (male, 67 years old with coronary heart disease and hypertension) at 37°C and muscle length amplitude oscillation of 0.125% produces a notch (labelled at 4.5 Hz). *C*, an MHC IIA human skeletal muscle fibre at 25°C and 5 mM P_i with a muscle length perturbation amplitude of 0.05% does not produce a notch. Sinusoidal length oscillations were applied from 0.25 to 200 Hz for each fibre type.

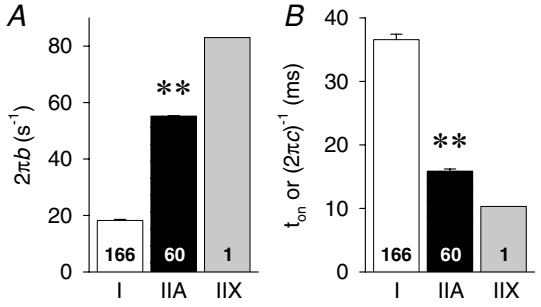

Figure 4. Fibre type differences in single human skeletal muscle fibre kinetic parameters
$2\pi b$ (*A*) and t_{on} (*B*) for Ca^{2+}-activated (pCa 4.5) skeletal muscle fibres expressing single MHC isoforms where controls (MHC I, $n = 86$; MHC IIA, $n = 28$) and heart failure patients (MHC I, $n = 80$; MHC IIA, $n = 32$; MHC IIX, $n = 1$) were combined. The number of fibres is indicated at the base of each bar. Conditions: 25°C and 5 mM P_i. Muscle length perturbation amplitude = 0.05%. Bar graphs represent mean ± S.E.M. $^{**}P < 0.01$ compared to MHC I.

curve fitting accuracy (seen graphically in Fig. 1*A*), we conclude this simplification was justified and does not qualitatively alter our conclusions regarding the primary effects of heart failure.

To demonstrate the utility of sinusoidal analysis to probe cross-bridge kinetics, we pooled the heart failure and control data to evaluate the effect of fibre type. We found $2\pi b$ increases and t_{on} decreases moving from slow to fast MHC isoforms (MHC I to IIA to IIX), as shown in Fig. 4. MHC IIA had higher ($P < 0.01$) $2\pi b$ and lower ($P < 0.01$) t_{on} compared to MHC I. Statistical differences for pure MHC IIX fibres could not be performed because only one was identified from the 227 fibres tested.

Single muscle fibre Ca^{2+}-activated elastic and viscous moduli across muscle oscillation frequencies for MHC I and IIA fibres are shown in Fig. 5. The shape of the elastic and viscous moduli are similar between MHC I and IIA, but are shifted to lower frequencies in MHC I compared to MHC IIA, as expected, due to the slower cross-bridge kinetic properties of MHC I. In both MHC I and IIA fibres, heart failure patients exhibit a leftward shift in portions of the elastic and viscous moduli curves compared to controls, indicating a slowing of cross-bridge kinetic properties. Specifically, heart failure patients have increased ($P < 0.05$) elastic moduli at frequencies slightly above the smallest elastic modulus value in both MHC I (3.5 to 8 Hz) and MHC IIA (10 to 25 Hz) fibres (Fig. 5*A* and *C*). Patients also have increased ($P < 0.05$) viscous moduli at frequencies slightly above the lowest viscous modulus value in both MHC I (1.75 to 4 Hz) and MHC IIA (6 to 12 Hz), and decreased ($P < 0.05$) viscous modulus at high frequencies in both MHC I (5.5 to 200 Hz) and MHC IIA (16 to 130 Hz) (Fig. 5*B* and *D*). Heart failure patients have a larger negative viscous modulus over a portion of their frequency range in both MHC I (0.6–0.8 Hz) and MHC IIA (3–4 Hz) fibres compared to controls, which results in a larger oscillatory work production ($P < 0.01$) in heart failure patients (MHC I, control: 151 ± 11 mJ m^{-3} *vs.* HF: 278 ± 13 mJ m^{-3}; MHC IIA, control: 502 ± 36 mJ m^{-3} *vs.* HF: 685 ± 40 mJ m^{-3}). The viscous modulus differences between patients and controls show a similar pattern

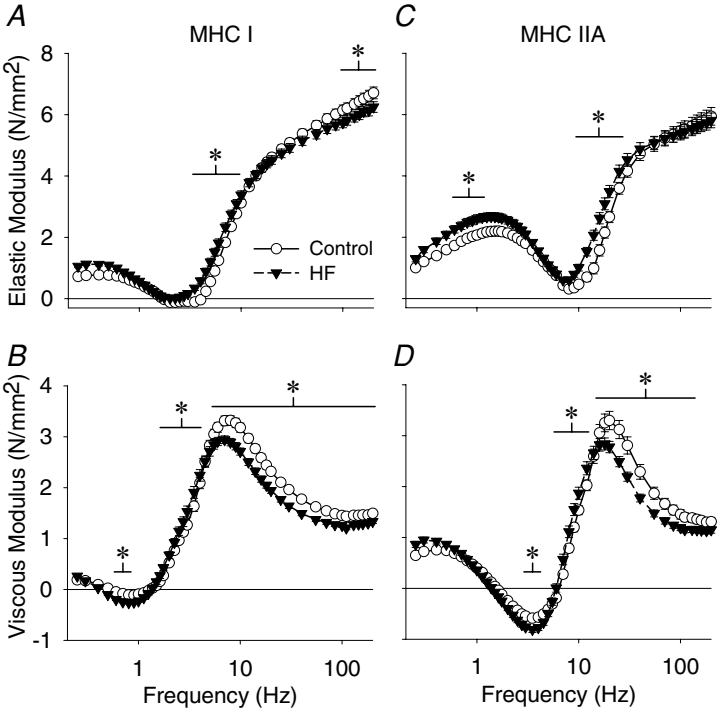

Figure 5. Elastic and viscous moduli response for Ca^{2+}-activated (pCa 4.5) MHC I and IIA fibres in heart failure and controls
Elastic and viscous moduli for MHC I (*A* and *B*) and MHC IIA (*C* and *D*) single human skeletal muscle fibres across muscle oscillation frequencies for controls (MHC I, $n = 87$; MHC IIA, $n = 28$) and heart failure patients (MHC I, $n = 85$; MHC IIA, $n = 32$). The notch, which occurs between 1–4 Hz in MHC I fibres and is easily identified in individual traces (Fig. 3*A*), is less noticeable when data are presented as group averages, due to the fact that the notch occurs at a variety of frequencies. Conditions: 25°C and 5 mM P_i. Muscle length perturbation amplitude = 0.05%. Values represent mean ± S.E.M. $^{*}P < 0.05$.

in MHC I and IIA fibres; however, the elastic modulus values for heart failure have some additional changes, with a decrease ($P < 0.05$) at high frequencies in MHC I (100–200 Hz) and an increase ($P < 0.05$) at low frequencies in MHC IIA (0.600–1.125 Hz) compared to controls.

The six parameters used to fit the complex modulus for MHC I (Fig. 6) and MHC IIA (Fig. 7) fibres exhibited similar differences between heart failure and controls. Examining the A-process parameters, *A* increased (Figs 6*A* and 7*A*, $P < 0.01$) and *k* decreased (Figs 6*B* and 7*B*, $P < 0.01$) with heart failure in MHC I and IIA. The magnitude portion of the B-process (*B*) and the C-process (*C*) remained unchanged in MHC I (Fig. 6*C* and *E*) and IIA (Fig. 7*C* and *E*) fibres with heart failure. The rate constant of the B-process, $2\pi b$, decreased ($P < 0.01$) with heart failure for MHC I (Fig. 6*D*) and MHC IIA (Fig. 7*D*) fibres, in agreement with the increased elastic and viscous moduli over a range of frequencies above their minimum values that occur with heart failure (Fig. 5*B* and *D*). The rate constant of the C-process, $2\pi c$, decreased with heart failure for MHC I (control: $30.7 \pm 0.7\ s^{-1}$ *vs.* HF: $28.1 \pm 0.9\ s^{-1}$; $n = 86$ and 80 fibres, $P < 0.05$) and MHC IIA (control: $70.4 \pm 1.5\ s^{-1}$ *vs.* HF: $59.2 \pm 1.4\ s^{-1}$; $n = 28$ and 32 fibres, $P < 0.01$). Thus, the average myosin attachment time, t_{on}, calculated using $(2\pi c)^{-1}$ was found to be increased ($P < 0.01$) with heart failure in both the MHC I (Fig. 6*F*; control: 34.2 ± 0.9 ms *vs.* HF: 39.1 ± 1.4 ms) and MHC IIA (Fig. 7*F*; control: 14.4 ± 0.3 ms *vs.* HF: 17.2 ± 0.4 ms) fibres.

MLC composition

The relative MLC composition of single MHC IIA fibres was examined as a potential explanation for the increased t_{on} with heart failure, as suggested by prior studies (Bottinelli *et al.* 1994). In the single fibres examined, only three isoforms of the myosin light chains, 1f, 2f and 3f, were observed. Expression of the fast essential or alkali light chains (Fig. 8*A*) was the same between controls and patients, although MLC 1f differences approached significance ($P = 0.06$). t_{on} did not correlate with essential light chain expression using a variety of MLC ratios. For example, no correlation was observed between t_{on} and MLC 3f/2f ratio (Fig. 8*B*; $P = 0.76$). Notably, t_{on} was increased in this sub-set of fibres with heart failure (control: 14.2 ± 0.4 ms *vs.* HF: 17.1 ± 0.4 ms; $n = 13$ and 24 fibres), similar to the larger sample of MHC IIA fibres (Fig. 7*F*). In addition, the essential light chain composition did not correlate with the other rate constant, $2\pi b$ ($P = 0.98$ for MLC 3f/2f ratio).

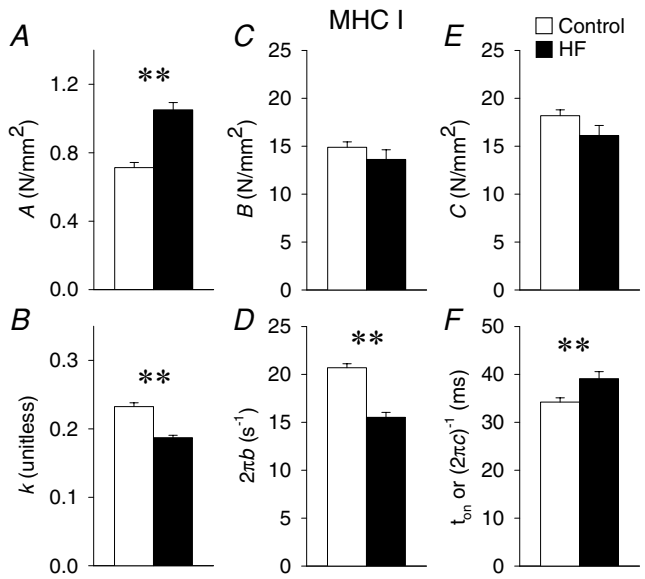

Figure 6. Sinusoidal analysis model parameter response for Ca^{2+}-activated (pCa 4.5) MHC I fibres in heart failure and controls

A- (panels *A* and *B*), B- (panels *C* and *D*) and C-process (panels *E* and *F*) parameters for Ca^{2+}-activated single MHC I skeletal muscle fibres for controls ($n = 86$) and heart failure patients ($n = 80$). Conditions: 25°C and 5 mM P_i. Muscle length perturbation amplitude = 0.05%. Bar graphs represent mean ± S.E.M. $^{**}P < 0.01$.

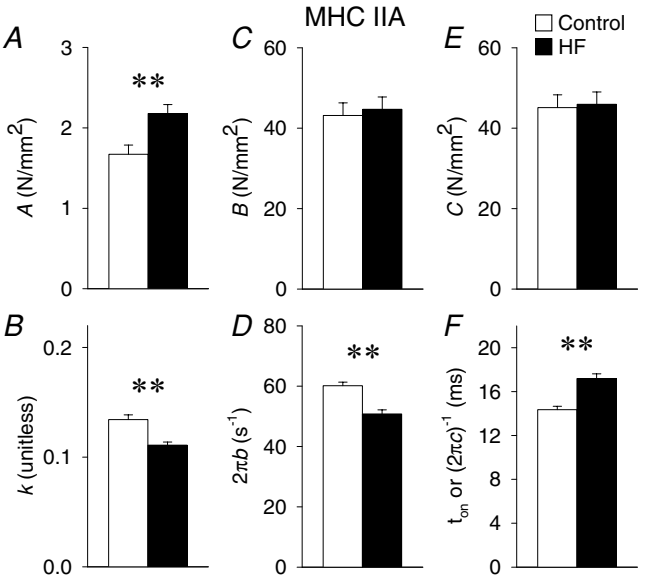

Figure 7. Sinusoidal analysis model parameter response for Ca^{2+}-activated (pCa 4.5) MHC IIA fibres in heart failure and controls

A- (panels *A* and *B*), B- (panels *C* and *D*) and C-process (panels *E* and *F*) parameters for Ca^{2+}-activated single MHC IIA skeletal muscle fibres for controls ($n = 28$) and heart failure patients ($n = 32$). Conditions: 25°C and 5 mM P_i. Muscle length perturbation amplitude = 0.05%. Bar graphs represent mean ± S.E.M. $^{**}P < 0.01$.

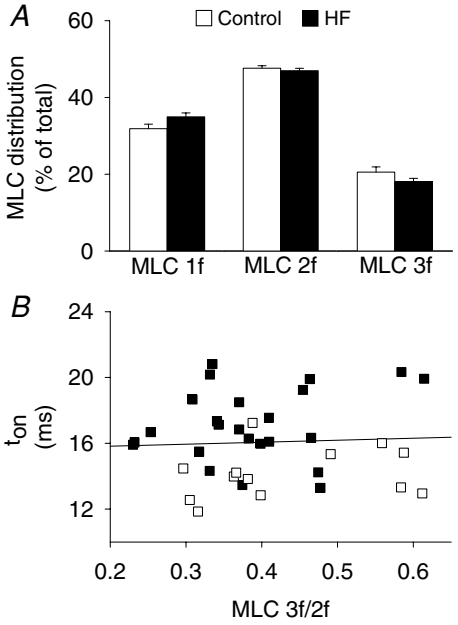

Figure 8. Relative MLC isoform distribution and relationship to t_{on} from MHC IIA fibres in heart failure and controls
Relative MLC isoform distribution (*A*) and relationship between t_{on} and MLC 3f/2f ratio (*B*) in single MHC IIA skeletal muscle fibres from controls ($n = 13$) and heart failure patients ($n = 24$). Regression line equation is $t_{on} = (1.22 * \text{MLC 3f/2f ratio}) + 15.58$ and has a $P = 0.76$. Bar graphs represent mean ± S.E.M.

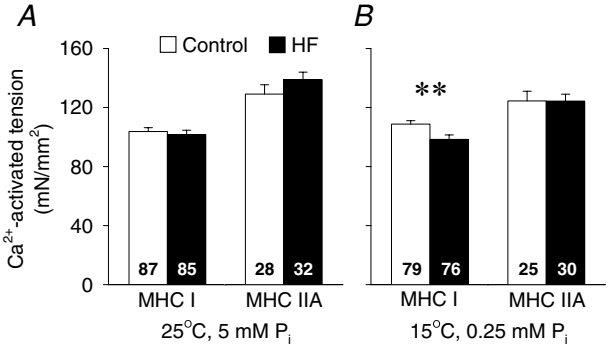

Figure 10. Ca^{2+}-activated (pCa 4.5) tension for MHC I and IIA fibres in heart failure and controls
Single skeletal muscle fibre Ca^{2+}-activated (pCa 4.5) tensions for MHC I and IIA fibres at 25°C and 5 mM P_i (*A*) and at 15°C and 0.25 mM P_i (*B*) in controls and heart failure patients. The number of fibres is indicated at the base of each bar. Bar graphs represent mean ± S.E.M. $^{**}P < 0.01$.

Ca^{2+} sensitivity

Normalized tension–pCa curves (15°C and 0.25 mM P_i) for MHC I and IIA fibres in heart failure patients and controls are shown in Fig. 9. In MHC I fibres, the pCa_{50} was unchanged in heart failure patients compared to controls (control: 5.74 ± 0.03 *vs.* HF: 5.69 ± 0.02; $n = 20$ and 22 fibres). In MHC IIA fibres, however, pCa_{50} was significantly lower in patients (control: 5.84 ± 0.02 *vs.* HF: 5.75 ± 0.02; $n = 11$ and 9 fibres, $P < 0.01$), indicating reduced Ca^{2+} sensitivity. The Hill coefficient did not differ between patients and controls for either MHC I (control: 2.98 ± 0.14 *vs.* HF: 2.64 ± 0.18) or MHC IIA (control: 3.32 ± 0.14 *vs.* HF: 3.75 ± 0.26).

Ca^{2+}-activated tensions

Single muscle fibre Ca^{2+}-activated tensions are shown in Fig. 10. Isometric tensions measured immediately prior to performing sinusoidal analysis (25°C and 5 mM P_i) were similar between patients and controls in MHC I and IIA fibres (Fig. 10*A*). Under conditions more typical for studies in human single muscle fibres (15°C and 0.25 mM P_i), patients showed lower tension in MHC I fibres ($P < 0.01$), while MHC IIA fibres remained similar to controls (Fig. 10*B*), in agreement with our previous report (Miller *et al.* 2009*b*).

Discussion

This study examined the effects of heart failure on single human skeletal muscle fibre function at the level of the myosin–actin cross-bridge and found alterations

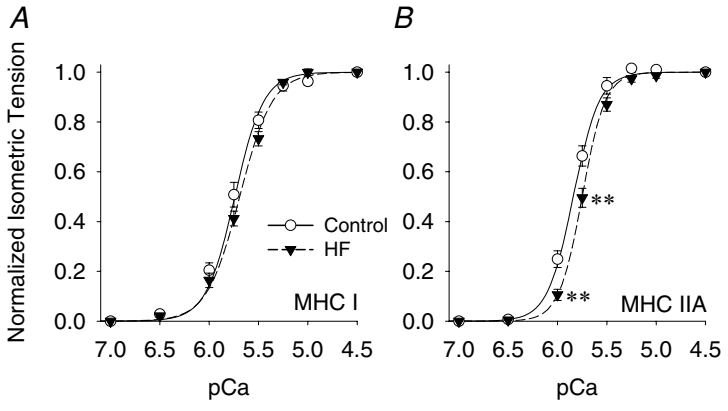

Figure 9. Tension–pCa relationship for MHC I and IIA fibres in heart failure and controls
Single skeletal muscle fibre isometric tension changes with Ca^{2+} concentration for MHC I (*A*) and MHC IIA (*B*) fibres from controls (MHC I, $n = 20$; MHC IIA, $n = 11$) and heart failure patients (MHC I, $n = 22$; MHC IIA, $n = 9$). Mean values for MHC I (pCa_{50}: control: 5.74 ± 0.03 *vs.* HF: 5.69 ± 0.02; *n*: control: 2.98 ± 0.14 *vs.* HF: 2.64 ± 0.18) and MHC IIA (pCa_{50}: control: 5.84 ± 0.02 *vs.* HF: 5.75 ± 0.02; *n*: control: 3.32 ± 0.14 *vs.* HF: 3.75 ± 0.26) fibres. Conditions: 15°C and 0.25 mM P_i. Values represent mean ± S.E.M. $^{**}P < 0.01$.

in cross-bridge kinetics, Ca^{2+}-activation and viscoelastic properties of the lattice structure compared to controls. These data are discussed within the context of prior results from our laboratory showing a loss of MHC protein content in fibres from heart failure patients (Toth *et al.* 2005; Miller *et al.* 2009*b*).

Application of sinusoidal length perturbation analysis to human muscle fibres

To our knowledge, this report represents the first application of the sinusoidal analysis technique to single human skeletal muscle fibres. While developing the sinusoidal analysis technique for application to human fibres, we uncovered a novel kinetic property of MHC I fibres, evident in the Nyquist plot as a 'notch' in the oscillatory frequency range between 1 and 4 Hz (Fig. 3*A*). This notch is not unique to MHC I skeletal muscle fibres, as we observe this phenomenon in human cardiac muscle strips (Fig. 3*B*), which primarily contain an identical isoform (β-MHC) to that in MHC I skeletal muscle fibres, and in embryonic isoforms of *Drosophila* muscle myosin (Yang *et al.* 2008). Thus, this phenomenon may be a fundamental characteristic of slow muscle myosins across species. While the mechanistic origin of the notch is unclear, preliminary modelling results suggest that two distinct populations of cross-bridges, one with a t_{on} that is greater than the other, cause two distinct force responses that lead to the notch. Solution studies using skeletal muscle MHC I support this interpretation and propose that under loaded conditions more longer-lived cross-bridges form, which may account for the enhanced contractile economy of MHC I fibres (Iorga *et al.* 2007). In intact skeletal muscle fibres, modulation of the fraction of cross-bridges in these two populations could have important physiological consequences.

The utility of sinusoidal analysis is evident in its ability to effectively define fibre type differences in cross-bridge kinetics. The general appearance of the elastic and viscous moduli and differences in moduli between MHC I and IIA (Fig. 5) agree well with results from rabbit fibres (Wang & Kawai, 1997; Galler *et al.* 2005). We found increases in $2\pi b$ and decreases in t_{on} as fibre type changes from MHC I to IIA to IIX (Fig. 4), indicating the rate constants of elementary steps of the cross-bridge cycle increase from MHC I to IIA to IIX, similar to rabbit skeletal muscle fibres (Wang & Kawai, 1997; Galler *et al.* 2005). To our knowledge, studies have only characterized cross-bridge kinetic parameters in human skeletal muscle fibres using quick stretch (Galler *et al.* 1997; Hilber & Galler, 1997; Hilber *et al.* 1999; Ochala *et al.* 2006) or release techniques (Ochala *et al.* 2007). These studies report that t_3, the time elapsed from the start of a stretch to the peak tension value of stretch activation, decreases from MHC I to IIA to IIX (Galler *et al.* 1997; Hilber & Galler, 1997; Hilber *et al.* 1999; Ochala *et al.* 2006), consistent with our findings of cross-bridge kinetics increasing from MHC I to IIA to IIX. Considering our subjects are elderly, physically inactive and include diseased individuals, we are careful not to draw generalized conclusions about fibre type differences in cross-bridge kinetics. Further studies in healthy young individuals are needed to clearly define 'normal' cross-bridge kinetics in single human skeletal muscle fibres.

Heart failure effects on single fibre cross-bridge kinetics

The most prominent change in single fibre skeletal muscle mechanics from heart failure patients is the slowing of cross-bridge kinetics in both MHC I and IIA fibres, indicated by the shift in portions of the elastic and viscous moduli to lower frequencies (Fig. 5) and the alterations in the curve fit parameters, specifically the increase in t_{on} (Figs 6*F* and 7*F*). Consistent with our results, slower overall cross-bridge kinetics have been found in the diaphragm muscle of rats with heart failure by measuring the rate of force redevelopment (van Hees *et al.* 2007). Our results extend these findings by measuring slower overall cross-bridge kinetics in single skeletal muscle fibres from human heart failure patients and by identifying a transition rate of the cross-bridge cycle that is altered, t_{on}.

Sinusoidal analysis, performed under isometric conditions at 25°C and 5 mM P_i, revealed an increased t_{on} in MHC I and IIA fibres from heart failure patients compared to controls, which has important consequences for single fibre function. Single fibre isometric tension in Ca^{2+}-activated fibres is directly related to the number of heads strongly bound to actin and the force generated per cross-bridge (Huxley, 1957; Brenner, 1988). Importantly, the number of heads strongly bound to actin is a function of the total population of available myosin heads multiplied by the fraction of the total cycle time myosin is bound to actin, or myosin duty ratio ($t_{on}/[t_{on}$ + myosin detachment time (t_{off})]). The loss of 17–36% MHC content previously observed in MHC I and IIA fibres from heart failure patients (Toth *et al.* 2005; Miller *et al.* 2009*b*) should decrease the total population of available myosin heads, leading to a decreased force-generating ability of single fibres. Surprisingly, heart failure patients and controls have similar single fibre isometric tensions within MHC I and IIA fibre types (Fig. 10*A*). Our observation that the *B* and *C* coefficients (Figs 6 and 7), parameters that are proportional to the number of myosin heads strongly bound to actin (Kawai *et al.* 1993; Palmer *et al.* 2007), are similar between patients and controls within MHC I and IIA fibre types suggests that tension

is maintained because a similar number of myosin heads are strongly bound in each group per fibre type, despite the loss of MHC content in heart failure patients. Our explanation for this result is that an increased t_{on} in MHC I and IIA fibres from heart failure patients would increase the number of heads strongly bound to actin by increasing the myosin duty ratio, assuming the increases in t_{on} have a larger effect on the myosin duty ratio than any increases in t_{off}. Notably, our previous study showing no effect of heart failure on maximal force of isolated myosins using the *in vitro* motility assay (Okada *et al.* 2008) and our current findings indicating similar numbers of myosin heads are strongly bound in each group per fibre type suggest that an increase in force generation per cross-bridge is not likely responsible for the maintenance of tension between heart failure patients and controls. Based on these data, we hypothesize that alterations in cross-bridge kinetics observed in our study compensate for the loss of MHC content in MHC I and IIA fibres in heart failure patients by increasing the number of heads strongly bound to actin to values similar to controls to prevent a loss in single fibre force production.

In addition to alterations in t_{on}, we observed a 15–25% decrease in the characteristic rate of the B-process (i.e. $2\pi b$) in MHC I and IIA fibres from heart failure patients (Figs 6*D* and 7*D*), which provides further evidence of slower cross-bridge kinetics. Historically, $2\pi b$ has been thought to reflect the rate of myosin transition between the weakly- and strongly-bound states (Kawai *et al.* 1993; Zhao & Kawai, 1993; Galler *et al.* 2005). These studies indicate $2\pi b$ is proportional to the sum of the forward and reverse rate constants governing this transition and related to P_i affinity and the equilibrium constants that comprise portions of t_{on}, specifically MgADP and MgATP affinity as well as ATP isomerization. Given the current data set, it was not possible to identify the specific rate and/or equilibrium constants that change because P_i, MgATP and MgADP concentrations were not varied. Assuming the decrease in $2\pi b$ is due primarily to a decrease in the forward rate constant, t_{off} would effectively be increased in heart failure patients. Our findings of a similar number of myosin heads bound in patients and controls, despite the loss of MHC content with heart failure, suggests that the increases in t_{on} in patients have a larger effect on the myosin duty ratio than any increases in t_{off}.

We examined changes in myosin light chain (MLC) composition, which has been shown to modulate single fibre function and kinetics (Bottinelli *et al.* 1994; Andruchov & Galler, 2008), as a possible explanation for increased t_{on} with heart failure. We evaluated this possibility in MHC IIA fibres since a more robust relationship between MLC composition and single fibre function has been observed in MHC II fibres (Bottinelli *et al.* 1994) compared to MHC I (Reiser & Bicer, 2006). In agreement with prior work (Billeter *et al.* 1981), only the MLC 1f, MLC 2f and MLC 3 isoforms were found in MHC IIA fibres, suggesting that differences in cross-bridge kinetics cannot be explained by the expression of slow MLC isoforms (Andruchov & Galler, 2008). Additionally, no differences in MLC distribution between heart failure patients and controls were found and no correlation was observed between essential MLC composition and t_{on} (Fig. 8). Our results agree with prior studies in humans showing that variation in single muscle fibre function is not accompanied by altered MLC composition (Larsson & Moss, 1993) and extend these findings to show that MLC composition does not relate to cross-bridge kinetic parameters in MHC IIA fibres.

Our results raise interesting questions regarding the interaction of various molecular determinants of myofilament protein function to regulate overall single fibre contractile performance. Our prior data collected at 15°C and low P_i (0.25 mM) showed no effect of heart failure on isometric tension in MHC IIA fibres despite reduced MHC protein content, although we did observe reduced tension in MHC I fibres (Miller *et al.* 2009*b*). Interestingly, tension differences in MHC I fibres disappear (Fig. 10*A*) when measured at 25°C and phosphate levels that approximate resting *in vivo* levels (5 mM; Pathare *et al.* 2005), the conditions under which sinusoidal analyses are performed. Thus, as the experimental conditions more closely mimic the *in vivo* environment with respect to temperature and phosphate level, the functional effect of MHC protein depletion to reduce single fibre force production is diminished by alterations in cross-bridge kinetics. These results suggest that the functional impact of myosin loss, which has now been observed in a number of physiological and pathophysiological conditions in animal models (Haddad *et al.* 2003; Acharyya *et al.* 2004; van Hees *et al.* 2007) and humans (Larsson *et al.* 2000; D'Antona *et al.* 2003; Ottenheijm *et al.* 2006; Miller *et al.* 2009*b*), but has typically been assessed at lower temperatures and phosphate levels (12–15°C and 0.25 mM P_i), can be partially or completely offset by alterations in cross-bridge kinetics. A specific mechanistic explanation for these reciprocal changes in the molecular determinants of contraction as experimental conditions move closer to *in vivo* is not clear. We do not believe that differences in cross-bridge kinetics are related to specific alterations in myosin or thin filament protein function, based on our prior work showing no effect of heart failure on isolated myosins or thin filaments using the *in vitro* motility assay (Okada *et al.* 2008). Instead, we hypothesize that diminished thick filament stiffness, due to reductions in MHC protein content, explain the slower cross-bridge kinetics with heart failure. Decreased thick filament stiffness may decrease the load imparted to the strongly bound cross-bridge or may decrease the constraints on the ability of the myosin head to find

an actin binding site, either of which could allow for longer cross-bridge attachment and effectively increase t_{on}, although this requires further study.

Heart failure effects on the tension–pCa relationship

Heart failure reduced the pCa_{50} in MHC IIA fibres due to decreased tension generation at the lower Ca^{2+} concentrations (Fig. 9*B*); whereas no differences in the Hill coefficient were observed, and neither of these variables were altered in MHC I fibres (Fig. 9*A*). From a functional standpoint, decreased calcium sensitivity could amplify the reductions in calcium release (Perreault *et al.* 1993) to diminish skeletal muscle strength in heart failure patients (Harrington *et al.* 1997; Toth *et al.* In Press).

Heart failure effects on single fibre structure

The A-process, which primarily represents the viscoelastic properties of the underlying lattice structure, as well as a portion related to the attached myosin heads (Mulieri *et al.* 2002; Palmer *et al.* 2004), changes similarly in both MHC I and IIA fibres with heart failure. Heart failure increases *A*, the magnitude of the A-process, and decreases *k*, the angle of the A-process with the *x*-axis (Figs 1*B*, 6 and 7). Together, these data indicate the A-process has higher elastic modulus values throughout the oscillation frequency range, although the differences are larger at lower frequencies, and lower viscous modulus values at high frequencies in heart failure fibres compared to controls. Our previous work in cardiac muscle has shown that, as the Ca^{2+} concentration is increased, the number of attached myosin heads increases accordingly, leading to an increase in both *A* and *k* (Palmer *et al.* 2004). The *A* and *k* in heart failure skeletal muscle fibres change in opposite directions, suggesting that the mechanism driving these changes is not the addition or removal of myosin heads. Instead, alterations in the A-process with heart failure may arise from changes in the underlying lattice structure, such as titin, which can affect passive stiffness and active contractile properties in skeletal muscles (Prado *et al.* 2005).

In summary, our results show that cross-bridge kinetics in MHC I and IIA fibres are slowed in heart failure patients, due at least in part to an increase in myosin attachment time (t_{on}). The increase in t_{on} appears to compensate for the loss of MHC content by increasing the myosin duty ratio which results in a comparable number of strongly bound cross-bridges in patients and controls. As a result, isometric tension in MHC I and IIA fibres was similar between patients and controls, when measured under the same conditions as the muscle mechanics experiments, 25°C and resting *in vivo* P_i levels (5 mM; Pathare *et al.* 2005). Decreased calcium sensitivity of MHC IIA fibres and an apparent alteration of the underlying lattice structure of MHC I and IIA fibres were also found in patients, the former of which may conspire with reduced sarcoplasmic reticulum calcium release (Perreault *et al.* 1993) to reduce whole skeletal muscle strength. Considering that a number of physiological (i.e. ageing (D'Antona *et al.* 2003) and disuse (Haddad *et al.* 2003)) and pathophysiological conditions (Larsson *et al.* 2000; Acharyya *et al.* 2004; Ottenheijm *et al.* 2006; Miller *et al.* 2009*b*) share this phenotype of MHC depletion, further research is required to elucidate the complex interactions of quantitative and qualitative alterations in myofilament proteins on the contractile properties of single muscle fibres. Our observed changes are probably unique to heart failure, rather than being a consequence of ageing or disuse, since the age and physical activity level of patients and controls were matched. Additionally, because heart failure patients were clinically stable and had mild to moderate disease, it is unlikely that differences in single fibre mechanical properties are a consequence of end-stage disease, which can be characterized by deterioration of multiple organs and systemic disruption of normal physiological function. Finally, our studies provide a direct demonstration in single muscle fibres of a unique kinetic property of MHC I cross-bridges which may have important physiological consequences.

References

Acharyya S, Ladner KJ, Nelsen LL, Damrauer J, Reiser PJ, Swoap S & Guttridge DC (2004). Cancer cachexia is regulated by selective targeting of skeletal muscle gene products. *J Clin Invest* **114**, 370–378.

Ades PA, Savage PD, Cress ME, Brochu M, Lee NM & Poehlman ET (2003). Resistance training on physical performance in disabled older female cardiac patients. *Med Sci Sports Exerc* **35**, 1265–1270.

Andruchov O & Galler S (2008). Influence of fast and slow alkali myosin light chain isoforms on the kinetics of stretch-induced force transients of fast-twitch type IIA fibres of rat. *Pflugers Arch* **455**, 1165–1172.

Bean JF, Kiely DK, Herman S, Leveille SG, Mizer K, Frontera WR & Fielding RA (2002). The relationship between leg power and physical performance in mobility-limited older people. *J Am Geriatr Soc* **50**, 461–467.

Billeter R, Heizmann CW, Howald H & Jenny E (1981). Analysis of myosin light and heavy chain types in single human skeletal muscle fibers. *Eur J Biochem* **116**, 389–395.

Bottinelli R, Betto R, Schiaffino S & Reggiani C (1994). Unloaded shortening velocity and myosin heavy chain and alkali light chain isoform composition in rat skeletal muscle fibres. *J Physiol* **478**, 341–349.

Brenner B (1988). Effect of Ca^{2+} on cross-bridge turnover kinetics in skinned single rabbit psoas fibers: implications for regulation of muscle contraction. *Proc Natl Acad Sci U S A* **85**, 3265–3269.

Chase PB & Kushmerick MJ (1988). Effects of pH on contraction of rabbit fast and slow skeletal muscle fibers. *Biophys J* **53**, 935–946.

Coirault C, Guellich A, Barbry T, Samuel JL, Riou B & Lecarpentier Y (2007). Oxidative stress of myosin contributes to skeletal muscle dysfunction in rats with chronic heart failure. *Am J Physiol Heart Circ Physiol* **292**, H1009–H1017.

D'Antona G, Pellegrino MA, Adami R, Rossi R, Carlizzi CN, Canepari M, Saltin B & Bottinelli R (2003). The effect of ageing and immobilization on structure and function of human skeletal muscle fibres. *J Physiol* **552**, 499–511.

Galler S, Hilber K & Pette D (1997). Stretch activation and myosin heavy chain isoforms of rat, rabbit and human skeletal muscle fibres. *J Muscle Res Cell Motil* **18**, 441–448.

Galler S, Wang BG & Kawai M (2005). Elementary steps of the cross-bridge cycle in fast-twitch fiber types from rabbit skeletal muscles. *Biophys J* **89**, 3248–3260.

Godt RE & Lindley BD (1982). Influence of temperature upon contractile activation and isometric force production in mechanically skinned muscle fibers of the frog. *J Gen Physiol* **80**, 279–297.

Haddad F, Roy RR, Zhong H, Edgerton VR & Baldwin KM (2003). Atrophy responses to muscle inactivity. I. Cellular markers of protein deficits. *J Appl Physiol* **95**, 781–790.

Harrington D, Anker SD, Chua TP, Webb-Peploe KM, Ponikowski PP, Poole-Wilson PA & Coats AJ (1997). Skeletal muscle function and its relation to exercise tolerance in chronic heart failure. *J Am Coll Cardiol* **30**, 1758–1764.

Hilber K & Galler S (1997). Mechanical properties and myosin heavy chain isoform composition of skinned skeletal muscle fibres from a human biopsy sample. *Pflugers Arch* **434**, 551–558.

Hilber K & Galler S (1998). Improvement of the measurements on skinned muscle fibres by fixation of the fibre ends with glutaraldehyde. *J Muscle Res Cell Motil* **19**, 365–372.

Hilber K, Galler S, Gohlsch B & Pette D (1999). Kinetic properties of myosin heavy chain isoforms in single fibers from human skeletal muscle. *FEBS Lett* **455**, 267–270.

Huxley AF (1957). Muscle structure and theories of contraction. *Prog Biophys Biophys Chem* **7**, 255–318.

Iorga B, Adamek N & Geeves MA (2007). The slow skeletal muscle isoform of myosin shows kinetic features common to smooth and non-muscle myosins. *J Biol Chem* **282**, 3559–3570.

Kawai M, Saeki Y & Zhao Y (1993). Crossbridge scheme and the kinetic constants of elementary steps deduced from chemically skinned papillary and trabecular muscles of the ferret. *Circ Res* **73**, 35–50.

Larsson L, Li X, Edstrom L, Eriksson LI, Zackrisson H, Argentini C & Schiaffino S (2000). Acute quadriplegia and loss of muscle myosin in patients treated with nondepolarizing neuromuscular blocking agents and corticosteroids: mechanisms at the cellular and molecular levels. *Crit Care Med* **28**, 34–45.

Larsson L & Moss RL (1993). Maximum velocity of shortening in relation to myosin isoform composition in single fibres from human skeletal muscles. *J Physiol* **472**, 595–614.

Miller MS, Dambacher CM, Knowles AF, Braddock JM, Farman GP, Irving TC, Swank DM, Bernstein SI & Maughan DW (2009*a*). Alternative S2 hinge regions of the myosin rod affect myofibrillar structure and myosin kinetics. *Biophys J* **96**, 4132–4143.

Miller MS, VanBuren P, LeWinter MM, Lecker SH, Selby DE, Palmer BM, Maughan DW, Ades PA & Toth MJ (2009*b*). Mechanisms underlying skeletal muscle weakness in human heart failure: alterations in single fiber myosin protein content and function. *Circ Heart Fail* **2**, 700–706.

Moss RL (1979). Sarcomere length–tension relations of frog skinned muscle fibres during calcium activation at short lengths. *J Physiol* **292**, 177–192.

Mulieri LA, Barnes W, Leavitt BJ, Ittleman FP, LeWinter MM, Alpert NR & Maughan DW (2002). Alterations of myocardial dynamic stiffness implicating abnormal crossbridge function in human mitral regurgitation heart failure. *Circ Res* **90**, 66–72.

Ochala J, Dorer DJ, Frontera WR & Krivickas LS (2006). Single skeletal muscle fiber behavior after a quick stretch in young and older men: a possible explanation of the relative preservation of eccentric force in old age. *Pflugers Arch* **452**, 464–470.

Ochala J, Frontera WR, Dorer DJ, Van Hoecke J & Krivickas LS (2007). Single skeletal muscle fiber elastic and contractile characteristics in young and older men. *J Gerontol A Biol Sci Med Sci* **62**, 375–381.

Okada Y, Toth MJ & VanBuren P (2008). Skeletal muscle contractile protein function is preserved in human heart failure. *J Appl Physiol* **104**, 952–957.

Ottenheijm CA, Heunks LM, Hafmans T, Van Der Ven PF, Benoist C, Zhou H, Labeit S, Granzier HL & Dekhuijzen PN (2006). Titin and diaphragm dysfunction in chronic obstructive pulmonary disease. *Am J Respir Crit Care Med* **173**, 527–534.

Palmer BM, Fishbaugher DE, Schmitt JP, Wang Y, Alpert NR, Seidman CE, Seidman JG, VanBuren P & Maughan DW (2004). Differential cross-bridge kinetics of FHC myosin mutations R403Q and R453C in heterozygous mouse myocardium. *Am J Physiol Heart Circ Physiol* **287**, H91–H99.

Palmer BM, Suzuki T, Wang Y, Barnes WD, Miller MS & Maughan DW (2007). Two-state model of acto-myosin attachment-detachment predicts C-process of sinusoidal analysis. *Biophys J* **93**, 760–769.

Pathare N, Walter GA, Stevens JE, Yang Z, Okerke E, Gibbs JD, Esterhai JL, Scarborough MT, Gibbs CP, Sweeney HL & Vandenborne K (2005). Changes in inorganic phosphate and force production in human skeletal muscle after cast immobilization. *J Appl Physiol* **98**, 307–314.

Perreault CL, Gonzalez-Serratos H, Litwin SE, Sun X, Franzini-Armstrong C & Morgan JP (1993). Alterations in contractility and intracellular Ca^{2+} transients in isolated bundles of skeletal muscle fibers from rats with chronic heart failure. *Circ Res* **73**, 405–412.

Pinsky JL, Jette AM, Branch LG, Kannel WB & Feinleib M (1990). The Framingham Disability Study: relationship of various coronary heart disease manifestations to disability in older persons living in the community. *Am J Public Health* **80**, 1363–1367.

Prado LG, Makarenko I, Andresen C, Kruger M, Opitz CA & Linke WA (2005). Isoform diversity of giant proteins in relation to passive and active contractile properties of rabbit skeletal muscles. *J Gen Physiol* **126**, 461–480.

Reiser PJ & Bicer S (2006). Multiple isoforms of myosin light chain 1 in pig diaphragm slow fibers: correlation with maximal shortening velocity and force generation. *Arch Biochem Biophys* **456**, 112–118.

Szentesi P, Bekedam MA, van Beek-Harmsen BJ, Van Der Laarse WJ, Zaremba R, Boonstra A, Visser FC & Stienen GJ (2005). Depression of force production and ATPase activity in different types of human skeletal muscle fibers from patients with chronic heart failure. *J Appl Physiol* **99**, 2189–2195.

Toth MJ, Gottlieb SS, Fisher ML & Poehlman ET (1997). Skeletal muscle atrophy and peak oxygen consumption in heart failure. *Am J Cardiol* **79**, 1267–1269.

Toth MJ, Matthews DE, Ades PA, Tischler MD, VanBuren P, Previs M & LeWinter MM (2005). Skeletal muscle myofibrillar protein metabolism in heart failure: relationship to immune activation and functional capacity. *Am J Physiol Endocrinol Metab* **288**, E685–E692.

Toth MJ, Shaw AO, Miller MS, VanBuren P, LeWinter MM, Maughan DW & Ades PA (2010). Reduced knee extensor function in heart failure is not explained by inactivity. *Int J Cardiol* **143**, 276–282.

Trappe S, Gallagher P, Harber M, Carrithers J, Fluckey J & Trappe T (2003). Single muscle fibre contractile properties in young and old men and women. *J Physiol* **552**, 47–58.

van Hees HW, Van Der Heijden HF, Ottenheijm CA, Heunks LM, Pigmans CJ, Verheugt FW, Brouwer RM & Dekhuijzen PN (2007). Diaphragm single-fiber weakness and loss of myosin in congestive heart failure rats. *Am J Physiol Heart Circ Physiol* **293**, H819–H828.

Wang G & Kawai M (1997). Force generation and phosphate release steps in skinned rabbit soleus slow-twitch muscle fibers. *Biophys J* **73**, 878–894.

Wilson JR & Mancini DM (1993). Factors contributing to the exercise limitation of heart failure. *J Am Coll Cardiol* **22**, 93A–98A.

Yang C, Ramanath S, Kronert WA, Bernstein SI, Maughan DW & Swank DM (2008). Alternative versions of the myosin relay domain differentially respond to load to influence *Drosophila* muscle kinetics. *Biophys J* **95**, 5228–5237.

Yu B, Kienbacher T, Growney ES, Johnson ME & An KN (1997). Reproducibility of the kinematics and kinetics of the lower extremity during normal stair-climbing. *J Orthop Res* **15**, 348–352.

Zhao Y & Kawai M (1993). The effect of the lattice spacing change on cross-bridge kinetics in chemically skinned rabbit psoas muscle fibers. II. Elementary steps affected by the spacing change. *Biophys J* **64**, 197–210.

Author contributions

M.S.M., P.V.B., M.M.L., P.A.A., D.W.M. and M.J.T. contributed to the conception and design of the experiments. M.S.M., P.V.B., J.M.B., B.M.P. and M.J.T. performed data collection, analysis and/or interpretation. All authors drafted or critically revised the manuscript and approved the final version submitted.

Acknowledgements

We thank all the volunteers who dedicated their valuable time to these studies. This study was supported by grants from the National Institutes of Health HL-077418, HL-086902, AG-031303 and RR-00109. The content is solely the responsibility of the authors and does not necessarily represent the official view of the National Heart Blood and Lung Institute, National Institute on Aging, or National Institutes of Health.